Fermi National Accelerator Laboratory

FERMILAB-Pub-76/74-THY
August 1976

Diffractive Production Amplitudes for $\alpha_P > 1$

GIUSEPPE MARCHESINI [+]
Fermi National Accelerator Laboratory, Batavia, Illinois 60510
and
Argonne National Laboratory, Argonne, Illinois 60439

and

ELIEZER RABINOVICI
Fermi National Accelerator Laboratory, Batavia, Illinois 60510

ABSTRACT

Inelastic fully diffractive production cross-sections are studied within the framework of a spin model version of RFT for $\alpha_P > 1$. Exact results are obtained for very large α_P and D = 1, a semiclassical approximation is used to probe all other α_P and D = 2. Absorption corrections cause the processes to be peripheral in impact-parameter and to exhibit clustering in rapidity. s channel unitarity constraints are shown to hold and in particular the Finkelstein-Kajantie paradox is resolved for any $\alpha_P > 1$.

[+]Address after October 1, 1976: Istituto di Fisica, Universita di Parma, Italy.

I. INTRODUCTION

The study of hadronic diffraction scattering at high energy, small momentum transfer has acquired a suitable framework within Gribov's Reggeon Field Theory.[1] The problem is particularly interesting for an input pomeron with intercept α_0 above one.

It was shown that the region $\alpha_0 > 1$ is itself divided into two parts, partitioned by a critical intercept α_0 denoted α_c. For $\alpha_0 < \alpha_c$ the theory is simpl and its behavior is governed by the leading singularity--a pole below one. For $\alpha_0 = \alpha_c$ the character of the theory changes, this case has been studied extensively in the last years.[1, 2] It leads to a $(\log s)^{\eta}$ behavior for the total cross-section. Recently the knowledge of the theory has been expanded[3, 4] to encompass all $\alpha_0 > \alpha_c$. In this case the energy dependence saturates the Froissart bound, namely $\sigma_T \sim \log^2 s$. The method used to deal with the case $\alpha_0 > \alpha_c$ was a truncated lattice version of RFT, which was solved exactly in some limits. The fact that this version indeed describes the infrared properties of RFT (with triple pomeron couplings) is supported by the analysis in ref. (3, 4), which smoothly reproduces the known perturbation theory results and by the analysis[5] of the behavior of the truncated version near α_c.

In this paper we pursue the study of this model by evaluating the amplitudes for inelastic diffractive exclusive production. The interest in this study is two-fold: First, the RFT is not obviously by construction s channel unitary. The result that for <u>any</u> $\alpha_0 > \alpha_c$ all elastic partial waves are finitely bound seems already to indicate the existance of

necessary elements of elastic s-channel unitarity in the model. However well-behaved elastic amplitudes have led in past models to violation of s-channel unitarity via inelastic diffraction production. In particular this has been shown in Ref. 6. In the absence of a rigorous proof for the existence of s-channel unitarity, the resolution of the FK paradox[6] for $\alpha_0 > \alpha_c$ will serve as a strong indication for consistency with s-channel unitarity of RFT. For $\alpha_0 = \alpha_c$ it has already[7] been shown that the FK disease is removed.

The second point of interest is in high energy phenomenology; quantum numbers permitting, the first candidate to govern the asymptotic behavior of any fixed multiplicity cross-section is multipomeron exchange between the produced particles. Thus understanding the features of inelastic diffractive production will lead to predictions of the energy behavior and t distributions of exclusive cross-sections.

The results of our calculations show that although α_0 is larger than α_c, due to the absorptive corrections, the energy behavior of each σ_n will eventually become constant. There exists a finite range of coupling constants of the produced external particle for which the FK paradox is resolved (this coincides with the result[7, 8] obtained for $\alpha = \alpha_c$).

In that case the total contribution of these processes to the total cross-section is energy independent while the total cross-section (as obtained from the elastic amplitude) is actually increasing. Therefore the main bulk of production processes is coming from events which are not fully diffractive and should be described in the framework of CRFT.[9]

From the more phenomenological aspect, absorption has a strong impact on the particle distributions. It forces a very peripheral structure in impact parameter space and also clusters the produced particles in rapidity.

The structure of the paper is as follows: In the next section we first recall the results necessary for our calculations from ref. 3, 4. Next we obtain the truncated lattice representations of composite (local) operators; special attention is paid to the mass insertion operator, which is relevant for the definition[7, 8] of inelastic diffractive amplitudes. We then comment on the relation of the spin model to RFT. In Section 3 we present an exact result for the inelastic diffractive processes in the limiting case $\alpha_0 \to \infty$, and D = 1 (one transverse dimension). This result is generalized, in the framework of a semi-classical approximation,[4] to any α_0 and D = 2. In particular the smooth transition towards the perturbative regime at small α_0 is emphasized. Finally, in Section 5 we discuss the physical picture emerging for inelastic diffractive exclusive production. This qualitative discussion may be read separately.

We turn now to recall the results obtained for the elastic amplitude for $\alpha_0 > \alpha_c$.

II. SPIN MODEL AND PRODUCTION AMPLITUDES

In this section we recall the derivation of the spin model analogue of RFT together with the features which are needed for the present calculation. We then identify the operator of this model which corresponds to the mass insertion operator of RFT and which is relevant for the calculation of the inelastic diffractive amplitudes.

2.1) Spin Model Derivation and Green's Functions

The RFT Hamiltonian[1] in a lattice in the impact parameter space (intersite distance a) is

$$H = \sum_i H_i^{(0)} + \frac{\alpha'}{a^2} \sum_{(i,j)} q_i p_j \tag{2.1}$$

$$H_i^{(0)} = \mu q_i p_i - \lambda a^{-D/2} q_i (p_i + q_i) p_i \tag{2.2}$$

where (i, j) are next neighbor points in the $\underline{b}$ space lattice of D dimension; α' is the pomeron slope, λ is the (real) triple pomeron coupling and $\mu = \alpha_0 - 1$. The fields $p_i q_i$ are related to the Gribov fields by ($\vec{b}_j = \vec{j}a$)

$$p_j = i\, a^{D/2} \psi(\vec{b}_j) \quad , \quad q_j = i\, a^{D/2} \psi^+(\vec{b}_j) \quad , \tag{2.3}$$

where i is introduced to make the coupling in 2.2 real, and simplify the treatment of phases.

The procedure of Ref. 3 for attempting a solution of RFT was to first

solve the single site dynamics [i.e., $\alpha' = 0$ in 2.1] and then introduce the intersite interaction. The first step of this program is greatly simplified by the fact[10,11] that the two lowest states of the single site Hamiltonian $H_i^{(0)}$ are almost degenerate for large $\left(\frac{\mu}{\lambda}\right)$: the energy gap is $2\Delta \sim e^{-\frac{1}{2}\left(\frac{\mu}{\lambda}\right)^2}$ (here and in the following we will often neglect to write explicitly a. Recall, however, that $\lambda a^{-D/2}$ and α'/a^2 are dimensionless.) In fact in this case one can neglect all other higher excitations and approximate any (local) operator with the matrix elements on a base truncated at these two states. It was found[3,11] that the matrix elements of $H_i^{(0)}$ and the fields $p_i q_j$ have the form

$$H_i^0 = 2\Delta \begin{pmatrix} 0 & 0 \\ 0 & 1 \end{pmatrix} = 2\Delta \left(\frac{1 - \sigma_3}{2}\right)_i = 2\Delta Z_i \quad ,$$

$$p_i = \frac{\mu}{\lambda} \begin{pmatrix} 0 & -1 \\ 0 & 1 \end{pmatrix} = \frac{\mu}{\lambda} P_i \quad , \quad q_i = \frac{\mu}{\lambda} \begin{pmatrix} 0 & 0 \\ 1 & 1 \end{pmatrix} = \frac{\mu}{\lambda} Q_i \quad , \tag{2.4}$$

and the RFT Hamiltonian in 2.2 is approximated by the Hamiltonian

$$H = 2\Delta \sum_i Z_i + J \sum_{(i,j)} P_i Q_i \quad ,$$

$$J = \alpha' \left(\frac{\mu}{\lambda}\right)^2 a^{D-2} \quad , \tag{2.5}$$

which defines our spin system analogue model.

A feature of this model shown in ref. 3 is that the dynamical system undergoes a phase transition for $x = \frac{\Delta}{J} \equiv x_c$; for $x > x_c$ the ground state

$$\phi_0 \equiv \pi_i \begin{pmatrix} 1 \\ 0 \end{pmatrix}_i , \quad H\phi_0 = 0 , \quad p_i \phi_0 = 0 \tag{2.6}$$

is unique while for $x < x_c$ it is twofold degenerate. However even in this case ϕ_0 is one of the two ground states since $H\phi_0 = 0$ for any x. The phase transition is of second order type since the order parameter $\sigma(x)$, which turns out to be the transition element between the two ground states, vanishes for $x \to x_c$.

The spin system Hamiltonian in 2.6 is pseudoHermitian, in fact there exists a metric operator

$$M \equiv \pi_i \sigma_3^i , \tag{2.7}$$

such that

$$MP_iM = Q_i^+, \quad MQ_iM = P_i^+, \quad MHM = H^+ . \tag{2.8}$$

This entails that if ϕ is a right eigenstate of H, the corresponding left eigenstate is

$$\overline{\phi} = \phi^+ M . \tag{2.9}$$

(The existence of this operator is a consequence of the symmetry of RFT with respect to the p, q^+ interchange which corresponds to the beam-target interchange in the hadronic process.)

The important fact that ϕ_0 is an exact ground state for any x implies that there is an unambiguous definition for the Green's functions of the theory which satisfies cluster decomposition and is continuous in x. In

particular for the two point function we have

$$G(\vec{B}, Y) = -\langle \bar{\phi}_0 | P_i e^{-HY} Q_j | \phi_0 \rangle, \quad \vec{B} = (\vec{i} - \vec{j})a \quad . \tag{2.10}$$

Moreover this definition maintains the symmetry 2.9. (The normalization of the Green's functions is such that $G(\vec{B}, Y = 0) = 1$, so that the factors $\frac{\mu}{\lambda}$ are absorbed in the couplings with external particles.) A feature of this theory is that the other (n, m) Green's functions are just given by 2.10. In fact, in the truncated base for fixed n we have

$$p_i^n = \left(\frac{\mu}{\lambda}\right)^n P_i \ , \quad q_i^n = \left(\frac{\mu}{\lambda}\right)^n Q_i \tag{2.11}$$

neglecting terms of order $e^{-1/2(\mu/\lambda)^2}$. (This however is no longer[5] valid for $n \to \infty$.)

As explained before, we study in Section 3 the diffractive production amplitude for the particular case of $x = 0$ and $D = 1$. The reason for this calculation is that in this case, as shown in Ref. 4, the Green's functions of the theory can be exactly calculated. This is because the equation of motion of the box state (see Fig. 1)

$$\xi^{\ell, m} \equiv \prod_{i<\ell} x_0^i \prod_{i=\ell}^{m} x_1^i \prod_{i>m} x_0^i \quad ; \quad x_0^i = \begin{pmatrix} 1 \\ 0 \end{pmatrix}, \ x_1^i = \begin{pmatrix} 1 \\ -1 \end{pmatrix} \tag{2.12}$$

can be exactly integrated to give

$$e^{-Hy}\xi^{\ell,\ m} = \sum_{n=0}^{\infty}\sum_{n'=0}^{\infty} f_n(y) f_{n'}(y) \xi^{\ell-n,\ m+n'} \quad , \tag{2.13}$$

where $f_n(y)$ is a Poisson distribution centered at $n = Jy$,

$$f_n(y) = e^{-Jy}\frac{(Jy)^n}{n!} \quad . \tag{2.14}$$

In fact in the matrix element in 2.10 we have a state of this type

$$Q_j \Phi_0 = \phi_0 - \xi^{j,\ j} \quad , \tag{2.15}$$

and using 3.13 we have

$$G(B,\ Y) = \langle \bar{\phi}_0 P_i e^{-HY}\xi^{j,\ j} \rangle = \sum_{n=0}^{\infty}\sum_{n'=0}^{\infty} f_n(Y) f_{n'}(Y) \langle \bar{\phi}_0 P_i \xi^{j-n,\ j+n'} \rangle . \tag{2.16}$$

Noting that

$$P_i x_0^{\ i} = 0, \quad P_i x_1^{\ i} = x_1^{\ i} \quad , \tag{2.17}$$

in Ref. 4 it was obtained

$$G(B,\ Y) = \sum_{n=|i-j|}^{\infty} f_n(Y) \simeq \theta(JaY - |B|) \tag{2.18}$$

which is a disc of opacity 1 expanding in Y with velocity

$$v = Ja \quad . \tag{2.19}$$

This solution can be generalized for any D or for $x < x_c$. In fact, by using a semiclassical approximation[4] in which $x_c = 1$, one obtains that for any D and $x < 1$ the Green's function G is a disc expanding with velocity $v(x) = Ja(1-x)^{1/2}$ and opacity $\sigma^2(x)$ where $\sigma(x)$ is the order parameter. This semiclassical approximation will be used in Section 4 to compute in general the form of the diffractive production amplitudes.

In the large x region one can attempt a perturbative calculation and in the semiclassical approximation[4] the Green's function in 2.10 makes a transition to a Regge pole with intercept $\bar{\alpha}$

$$\bar{\alpha} - 1 = 2J(1-x) \quad , \tag{2.20}$$

smaller than one ($x > 1$) and slope $\bar{\alpha}'$

$$\bar{\alpha}' = Ja^2. \tag{2.21}$$

This fact gives further support to the conjecture already discussed that the spin model of Eq. 2.5 we are working with is intimately related to the full RFT and describes the interaction of Reggeons with parameters 2.20 and 2.21. It is not obvious, however, how the identification of these two parameters survives in the continuum limit of this spin model ($a \to 0$). We now further elaborate this point.

2.2) Relation of the Spin Model with RFT

All our calculations of fully diffractive cross sections will be done in the spin model of RFT which was derived in the large α_0 region or small λ. A

relevant question which arises is whether our results can be related to the features of RFT not only for large α_0 but for any α_0. The expectation we have is that the spin model has the same features of RFT for any α_0. This stems from the hope that the two theories belong to the same class of universality and that in the semiclassical approximation for $x > x_c$ the spin model describes interactions of Reggeons. However when we consider the continuum limit of the spin model a problem arises in the case $x > x_c$ i.e., α_0 is small. This is probably related to the improper treatment of ultraviolet divergences.

In the spin model there are two dimensionless parameters, J and $x = \Delta / J$, and the only parameter which sets the scale is the lattice size a, which in RFT plays the role of an ultraviolet cut off. This is due to the fact that the original dimensional parameters α' and λ enter in dimensionless combinations Δ and J once the truncation procedure in 2.4 is performed.

In the region $x < x_c$ the limit $a \to 0$ can be properly done. In fact in that case there is only one relevant parameter in the theory which is the velocity of the expansion of the disc $v = Ja$. In this case it is possible to maintain unchanged the dynamics of the system in the limit $a \to 0$ provided we keep $v(x)$ fixed in the limit. For $x > x_c$ (small α_0) instead the limit gives rise to a problem. In fact we have seen in the

semiclassical approximation that the spin model describes the interaction of Reggeons with intercept and slope given in 2.20, 2.21. It is clear that in this case these two relevant parameters cannot be kept fixed in the $a \to 0$ limit. This of course brings some shade on the relation of our results with RFT in the case $x > x_c$, even though it is comforting that we obtain formally a Regge pole.

2.3) Matrix Elements for Diffractive Production Amplitudes

Before entering the detailed computation let us briefly recall the type of RFT diagrams which describe the fully diffractive inelastic processes we are interested in. In absence of cuts, the amplitude is represented by the ladder-like diagrams of pure Pomeron exchanges (Fig. 2). When a triple pomeron coupling is turned on, one has to sum absorptive type diagrams such as in Fig. 3a, 3b and new type of production amplitudes such as Fig. 3c. In RFT the sum of all these diagrams are described[7,8] by the matrix element

$$G^{(n)}(\vec{B},\ Y;\ \vec{b}_\ell,\ y_\ell) = \langle 0 \left| \psi(\vec{B}, Y) \prod_{i=1}^{n} \psi^+(\vec{b}_i, y_i)\psi(\vec{b}_i, y_i)\psi^+(\vec{0},\ 0) \right| 0 \rangle \quad , \quad (2.22)$$

$$Y > y_n > \ldots > y_1 > 0 \quad ,$$

where y_i, $\vec{b}_i$ are the rapidity and impact parameters of produced particles.

In addition to these diagrams one has in general to consider the case in which more pomerons are attached to the external particles, as in the diagrams of Fig. 4. These contributions are described in RFT by the

matrix 2.22 where the fields $\psi^+(\vec{B},Y)$ and $\psi^+(\vec{0},0)$ are substituted by their powers. For $\alpha_0 > \alpha_c$ their contribution to the hadronic S matrix cannot be neglected, in fact in the spin model, due to the property of eq. 2.11, they are of the same order as $G^{(n)}$ (eq. 2.22). The full S-matrix is given by their infinite sum; it is complicated by the fact that eq. 2.11 does not hold for $n \to \infty$. It can be shown however that the sum is finite provided that the matrix in 2.22 is finite. For this reason in the following we consider only the matrix element in 2.22.

We want now to establish the form of the production amplitudes in the spin model. To this purpose we have to identify the operator of the model which corresponds to the mass insertion $\psi_i^+ \psi_i = -q_i p_i$ in 2.22. This can be obtained by computing in the truncated base of $H_i^{(0)}$ the matrix element of the local operator $q_i p_i$. In a way similar to the one for the calculation of 2.4 we obtain

$$\mu q_i p_i = 2\Delta\left(\frac{\mu}{\lambda}\right)^2 \begin{pmatrix} 0 & 0 \\ 0 & 1 \end{pmatrix} = 2\Delta\left(\frac{\mu}{\lambda}\right)^2 Z_i \quad . \tag{2.23}$$

Note that the truncated matrix of the operator $q_i p_i$ is not the product of the two truncated operators in 2.4. In fact $Q_i P_i = 0$. This means that in the matrix elements of $q_i p_i$ intermediate states with higher excitations are contributing to give the finite result 2.23.

The identification of the mass operator with Z_i in 2.23 is also consistent with the fact that for large x the spin Hamiltonian describes the interaction

of Reggeons with the intercept $\bar{\alpha}$ (2.20). The mass operator should then coincide with the operator which in the Hamiltonian is proportional to the parameter 2Δ, i.e., with Z_i.

With this identification the diffractive production amplitudes are given by the following matrix elements of the spin system

$$G^{(n)} = -\langle \phi_0 | P_i e^{-H(Y - y_n)} Z_{\ell_n} e^{-H(y_n - y_{n-1})} \ldots Z_{\ell_1} e^{-Hy_1} Q_0 | \phi_0 \rangle \qquad (2.24)$$

with $Y > y_n > \ldots > y_1 > 0$ and $\vec{b}_n = \vec{\ell}_n a$, $\vec{B} = \vec{i} a$. (Again the normalization is such that when all y's are zero $G^{(n)} = 1$. The coupling constants of the external particles have to be independently added)

III. PRODUCTION CROSS SECTIONS FOR $\Delta = 0$ AND $D = 1$: EXACT SOLUTION

In this section we compute the matrix elements 2.24 for the inelastic diffractive amplitudes in the special case $\Delta = 0$ and $D = 1$. Nature being at $D = 2$, one may wonder why to study this special case. The direct appeal in the $D = 1$ $\Delta = 0$ case is that the spin model can be exactly solved.[4] In any case the $x = 0$ limit would start to give us indications of the general features of these amplitudes in the $x < x_c$ region which will be investigated in the next section. Moreover, this case provides then the edge of the trend leading to the $x = x_c$ case and beyond, into the perturbation regime for $x > x_c$. From the point of view of satisfying s channel unitarity constraints,

it should be pointed out that the FK disease turns more acute the smaller D is and the larger α_0 is. Thus a resolution of the FK paradox for D = 1 strongly indicates that it is resolved also for large D.

The first case we consider is the inelastic production of one additional particle, for which the amplitude is

$$G^{(1)}(BY;\ by) = -\langle\bar{\phi}_0 \mid P_i\, e^{-H(Y-y)} Z_\ell\, e^{-Hy} Q_0 \mid \phi_0\rangle \tag{3.1}$$

with B = ia, b = ℓa. From eq. 2.15, 2.13 and its conjugate equation ($\bar{\xi} = \xi^+ M$) we obtain

$$G^{(1)} = -\sum_{n,\,n',\,m,\,m'=0}^{\infty} f_m(Y-y) f_{m'}(Y-y) f_n(y) f_{n'}(y) \langle\bar{\xi}^{i-m,\ i+m'} \mid Z_\ell \mid \xi^{-n,\ n'}\rangle \ , \tag{3.2}$$

where $f_n(y)$ is the Poisson distribution defined in 2.14. Since

$$Z_\ell x_0^{\ \ell} = 0, \quad Z_\ell x_1^{\ \ell} = x_1^{\ \ell} - x_0^{\ \ell} \ , \tag{3.3}$$

we can compute the matrix element in 3.2. In fact from 3.3 we have that ℓ should belong to the intervals $[i - m,\ i + m']$ and $[-n,\ n']$, and in this case Z_ℓ on the state ξ gives again ξ minus a state with a hole at ℓ. Moreover, taking into account that the scalar product (with the M metric in 2.9) of two box states is different from zero only if they do not overlap, we obtain

$$\langle \bar{\xi}^{i-m,\, i+m'} \,|\, Z_\ell \,|\, \xi^{-n,\, n'} \rangle = -\left(\delta_{\ell,\, i-m}\delta_{\ell,\, n'} + \delta_{\ell,\, i+m'}\delta_{\ell,\, -n}\right). \tag{3.4}$$

The meaning of this equation is clear: Z_ℓ has to act at the edges of the two box states ξ and $\bar{\xi}$ in the configuration in which they do not overlap (see Fig. 5). Finally for $G^{(1)}$ we obtain

$$G^{(1)}(B,Y;\, b,y) = f_{i-\ell}(Y-y)f_\ell(y) + f_{\ell-i}(Y-y)f_{-\ell}(y) \quad . \tag{3.5}$$

The meaning of this result becomes clearer if we go to the continuum limit of $a \to 0$ in which the Poisson distribution $f_n(y)$ turns into the Gaussian

$$f_n(y) \to \frac{e^{-(b-Jay)^2/2Ja^2y}}{(2\pi Ja^2y)^{1/2}} \tag{3.6}$$

which is centered around $b = Jay$. In order to have a meaningful limit we have to keep $v = Ja$ fixed. In this limit we have

$$G^{(1)}(B,Y;\, b,y) = \frac{e^{-(B-b-v(Y-y))^2/2Ja^2(Y-y)}}{(2\pi Ja^2(Y-y))^{1/2}} \frac{e^{-b^2/2Ja^2y}}{(2\pi Ja^2y)^{1/2}} + (B \to -B,\ b \to -b). \tag{3.7}$$

Here is a first sign of a peculiar difference between elastic and inelastic diffractive amplitudes. While for the elastic amplitudes the two particles interact for <u>any</u> impact parameter B in the disc $B^2 \le v^2Y^2$ (see eq. 2.18), in the inelastic case the amplitude is <u>peripheral</u>. For a given Y and y the

inelastic amplitude is different from zero only for

$$b \simeq vy, \quad B \simeq vY \qquad \text{or} \qquad b \simeq -vy, \; B \simeq -vY \quad . \tag{3.8}$$

Outside this region in b and B the amplitude $G^{(1)}$ drops to zero with a Gaussian tail. We will see that this peripheral structure persists in higher multiplicity cross-sections and it is actually this depletion of the available production phase space which cures the FK disease.

The next step is to calculate the rapidity differential cross section. The integration (or summation) over the impact parameter phase space leads to

$$\frac{d\sigma^{(1)}}{dy} = \int dB\, db\, |G^{(1)}|^2 = \sum_i \sum_\ell |G^{(1)}|^2 = e^{-2JY} I_0\big(2J(Y-y)\big) I_0(2Jy) \tag{3.9}$$

We note the following points:

(1) $I_0(x)$ is finite for $x = 0$, and behaves for large x like

$$I_0(x) \xrightarrow[x \to \infty]{} \frac{e^x}{\sqrt{x}} \quad .$$

For large rapidities differences, we will therefore have

$$\frac{d\sigma}{dy} \approx \frac{1}{\sqrt{y}} \; \frac{1}{\sqrt{Y-y}} \tag{3.10}$$

and consequently the "middle" particle tends to be produced near one of the leading particles.

(2) Having a simple factorizing form in the t channel after all types of triple-pomeron absorptions are taken into account is rather surprising. If the generalization to n particle production would be

$$\frac{d\sigma}{dy_1 \ldots dy_n} = \prod_{i=2}^{n} I_0[2J(y_i - y_{i-1})] ,$$

a violation of s channel unitarity would be imminent. It will turn out that factorization will indeed be achieved but the object iterated in the t channel will not be function I_0.

The total σ_3 can be calculated exactly in this case and is given by

$$\sigma_3 = 2e^{-Jy} \sin 2Jy. \tag{3.11}$$

The cross-section which before addition of cuts increases like $s^{\alpha_0 - 1}$ has been tamed and increases toward a constant.

Let us now consider the general inelastic amplitude $G^{(n)}$ in 2.24. This expression and its evaluation can be simplified noticing that if $B > 0$ ($B < 0$) only the evolution of the right (left) edge of the box in $Q_0 \phi_0$ (eq. 2.15) is relevant in the evaluation of the Green's functions. This can be deduced from the discussion of eq. 3.4. Similarly if $B > 0$ ($B < 0$) only the left (right) edge of the conjugate box in $\bar{\phi}_0 P_i$ is relevant. This suggests to introduce the states[4]

$$R^{\ell} = \prod_{i \le \ell} x_1^i \prod_{i > \ell} x_0^i , \quad L^{\ell} = \prod_{i < \ell} x_0^i \prod_{i \ge \ell} x_1^i \tag{3.12}$$

which allows to write for $B > 0$

$$G^{(n)}(B,Y;\, b_\ell y_\ell) = -\langle \bar{L}^i e^{-H(Y - y_n)} Z_{\ell_n} e^{-H(y_n - y_{n-1})} \ldots Z_{\ell_1} e^{-Hy_1} R^0 \rangle \quad (3.13)$$

where $B = ia$, $b_k = \ell_k a$. For $B < 0$ we have to interchange L and R. The evaluation of $G^{(n)}$ is essentially simplified by the observation that, as was the case in 3.4, the operator Z_ℓ should act only at the border of the disc. Namely, in the evaluation of the state in 3.13 (see Ref. 4).

$$e^{-H(y_2 - y_1)} Z_{\ell_1} e^{-Hy_1} R^0 = \sum_{m=0}^{\infty} f_{\ell_1 + m}(y_1) e^{-H(y_2 - y_1)} Z_{\ell_1} R^{\ell_1 + m}, \quad (3.14)$$

only the term $m = 0$ gives the relevant contribution. In fact we show in the Appendix that the rest of the sum evolves to zero like $e^{-2J(y_2 - y_1)}$ and furthermore contributes to the matrix element of $G^{(n)}$ with the tail of the Poisson distribution which provides an extra $e^{-J(y_2 - y_1)}$ coupling. We can neglect these contributions on the basis that in the continuum limit $a \to 0$ we have instead to maintain $v = Ja$ fixed so that $e^{-3J(y_2 - y_1)} \to 0$. In any case even for a finite these exponential contributions are of the type of nonleading Regge pole exchanges.

By using the fact that only $m = 0$ in 3.14 is contributing and taking into account 3.3 we obtain

$$e^{-H(y_2 - y_1)} Z_{\ell_1} e^{-Hy_1} R^0 \simeq f_{\ell_1}(y_1) e^{-H(y_2 - y_1)} \left(R^{\ell_1} - R^{\ell_1 - 1}\right) \tag{3.15}$$

$$\simeq f_{\ell_1}(y_1) \sum_{n=0}^{\infty} \left[f_n(y_2 - y_1) - f_{n-1}(y_2 - y_1)\right] R^{\ell_1 + n} .$$

It is clear that this mechanism generalizes in the evaluation of $G^{(n)}$ and gives

$$G^{(n)}(B,Y;\, b_\ell y_\ell) = f_{i - \ell_n}(Y - y_n) \prod_{k=2}^{n} \Delta f_{\ell_k - \ell_{k-1}}(y_k - y_{k-1}) f_{\ell_1}(y_1) \tag{3.16}$$

$$+ (i \to -i,\ \ell_k \to -\ell_k) \quad ,$$

where $\Delta f_n(y)$ is the difference of the two Poisson distribution centered at $n = Jy$, $n = Jy + 1$,

$$\Delta f_n(y) = f_n(y) - f_{n-1}(y) \quad , \tag{3.17}$$

which in the continuum limit becomes

$$\Delta f_n(y) \to \frac{(b - vy)}{vy} \frac{e^{-(b - vy)^2 / 2Ja^2 y}}{(2\pi Ja^2 y)^{1/2}} \quad . \tag{3.18}$$

The physical meaning of this result for $G^{(n)}$ is the following. The inelastic diffractive amplitudes are different from zero only for

$$B \simeq vY,\ b_\ell \simeq vy_\ell \qquad \text{for } B > 0,$$
$$B \simeq -vY,\ b_\ell \simeq -vy_\ell \qquad \text{for } B < 0. \tag{3.19}$$

All impact parameters are aligned and an ordering in rapidity implies an ordering in impact parameter. Outside this region the amplitudes $G^{(n)}$ drop to zero with a Gaussian tail. The fact that the produced particles are very rigid in their impact parameter positions will again be the key to the resolution of the FK paradox.

The rapidity differential cross sections are given from 3.15

$$\frac{d\sigma}{dy_1 \dots dy_n} = \int dB\, db_1 \dots db_\ell \left| G^{(n)} \right|^2 = \sum_i \sum_{\ell_1} \cdots \sum_{\ell_n} \left| G^{(n)} \right|^2 = \tag{3.20}$$
$$e^{-2JY} I_0(2J(Y - y)) \prod_{i=2}^{n} F(y_i - y_{i-1}) I_0(2Jy_1)$$

where

$$F(y) = I_0(2Jy) - I_1(2Jy). \tag{3.21}$$

The factorized form is indeed maintained even in the presence of absorptive processes. However the object iterated in the t channel is F(y) and not I_0. The crucial difference is that for large rapidity separation

$$e^{-2Jy} F(y) \to \frac{1}{y} \frac{1}{\sqrt{y}}, \tag{3.22}$$

so that

$$\frac{d\sigma}{dy_1 \cdots dy_n} \alpha \frac{1}{(Y - y_n)^{1/2}} \prod_{i=2}^{n} \frac{1}{(y_i - y_{i-1})^{3/2}} \frac{1}{(y_1)^{1/2}} . \qquad (3.23)$$

The extra factor $1/y$ has striking physical consequences. It causes the rapidity difference between each two adjoint inelastically produced particles to remain finite. They will form a cluster which will tend itself (as we learn from the $G^{(1)}$ case) to cluster near one of the two leading particles. The physical prediction of the unimportance of the many large-gap type processes, is a unique feature of RFT generated dynamically by absorption. The additional depletion of phase space (this time reflected in the longitudinal part) leads to constant n-particle production cross-sections. This can be estimated by integrating eq. 3.20. In fact the Laplace transform of $\sigma_n(Y)$, obtained from 3.20, is given by

$$\tilde{\sigma}_n(E) \alpha g^{2n} \frac{1}{s^2} \left[\frac{s - E}{s(s + p)}\right]^n , \qquad (3.24$$

where $p = 2J - E$, $s = (E(E - 4J))^{1/2}$, $E < 0$, and a coupling g^2 for producing particles has been introduced. Thus all $\sigma_n(Y)$ are asymptotically constants.

The total sum of these diffractive cross sections is obtained from

$$\hat{\sigma}(E) \propto \frac{1}{s^2} \frac{s(s+p)}{s(s+p) - g^2(s-E)} \simeq \frac{1}{E} \frac{1}{2J - g^2} \tag{3.25}$$

which leads to a constant as long as $g^2 < 2J$. These fully diffractive processes not only do not violate s channel unitarity, thus resolving the FK paradox, but their relative ratio to the total cross section is vanishing asymptotically. One can also calculate the average multiplicity of these processes by taking the derivative of $\hat{\sigma}(E)$ with respect to g, it turns out that the average multiplicity is constant. This supports the view we discussed in the Introduction that the main bulk of the inelastic processes is not diffractive, and particles are mainly produced in short range type of processes or intermediate state of the bare pomerons as is described by the cut Reggeon Field Theory.[9]

A subtle question may arise due to the fact that we have neglected non-leading terms vanishing in the $a \to 0$ limit (see Appendix). One may wonder whether the limit $a \to 0$ commutes with the sum over all produced particles, giving rise to the suspicion that the sum over the neglected terms may give the leading output result (as is the case in the original FK treatment). However there are some features which distinguish this case. Beginning from a "bare" cross-section behaving like $s^{\alpha_0 - 1}$, we reach constant $\sigma_n(s)$

thus obtaining in any case a very large negative renormalization, on top of it all non-leading terms omitted in the calculation were non-leading by powers and not by logarithms. The leading form itself does not contain a signal for a possible violation (unlike the usual FK case). All this leads us to trust a summation within the framework of our spin model. For $\alpha_0 = \alpha_c$ this problem has been solved[7] and also there no new singularity occurs.

After studying in detail this case we turn to discuss the modifications occuring for $D \neq 1$, $x \neq 0$.

IV. PRODUCTION CROSS SECTION FOR $\Delta \neq 0$, $D \neq 1$: SEMICLASSICAL APPROXIMATION

For $\Delta \neq 0$ and/or $D \neq 1$ we have no explicit solution. In the case $D = 1$ and $x = \Delta/J$ small ($x < x_c$) a perturbative calculation can be done around the solution $x = 0$. In $D = 2$ the problem becomes far more complicated. Instead of proceeding with this study, in this section we compute the production amplitudes using the semiclassical approximation introduced in Ref. 4, which presumably leads at least to a qualitative understanding of the general features.

Let us start by recalling the semiclassical approximation for the functional state

$$\phi[\{\sigma_i\}] \equiv \prod_i x^i_{\sigma_i} \quad , \quad x_\sigma = \begin{pmatrix} 1 \\ -\sigma \end{pmatrix} , \tag{4.1}$$

with

$$(\bar{\phi}_0 \phi[\sigma]) = 1$$

$$(\bar{\phi}_0 P_\ell \phi[\sigma]) = \sigma_\ell \tag{4.2}$$

$$(\bar{\phi}_0 P_\ell P_{m'} \phi[\sigma]) = \sigma_\ell \sigma_m \qquad \ell \neq m.$$

If one makes the approximation[4] of neglecting correlations in the time evolution, i.e.,

$$\left(\bar{\phi}_0 P_\ell P_m e^{-HY} \phi[\sigma]\right) \simeq \left(\phi_0 P_\ell e^{-HY} \phi[\sigma]\right)\left(\phi_0 P_m e^{-HY} \phi[\sigma]\right), \quad \ell \neq m \ , \tag{4.3}$$

we have the following time evolution equation for the state in 4.1

$$e^{-Hy} \phi\left[\{\sigma_i\}\right] \simeq \phi\left[\{\sigma_i(y)\}\right] \ , \tag{4.3}$$

where $\sigma(\vec{b}, y) = \sigma_i(y)$ satisfies the classical equation

$$\frac{\partial}{\partial y} \sigma(b,y) = 2J\sigma(b,y)\left[1 - x - \sigma(b,y)\right] + (1 - \sigma(b,y)) Ja^2 \nabla_b^2 \sigma(b,y) \ . \tag{4.4}$$

Before passing to the calculation of the production amplitudes we recall also the feature of the solution of 4.4. The critical value x_c turns out to be $x_c = 1$. For $x > 1$ the relation at large y behaves as a Regge pole propagator with intercept $1 + 2J(1 - x)$ smaller than one

$$\sigma(b,y) \approx e^{2J(1-x)} \frac{e^{-b^2/2Ja^2y}}{(Ja^2y)^{D/2}} \qquad x > 1 \ , \tag{4.5}$$

the slope being Ja^2. For $x < 1$, $\sigma(b,y)$ is a disc with opacity $\sigma(x) = 1 - x$ and expanding with velocity $v(x) = Ja\sqrt{1 - x}$:

$$\sigma(b,y) \simeq \sigma(x) = 1 - x \quad \text{for } b^2 < v^2(x)y^2, \quad x < 1 \ . \tag{4.6}$$

At large b, $\sigma(b, y)$ vanishes matching the perturbative solution in 4.5, i.e., with a Gaussian tail. We obtain then for $x = 0$, $D = 1$ the same feature of the expanding box states we have discussed in the previous section.

Given the time evolution of the states in 4.1 we are now in position of computing the diffractive production amplitudes in 2.24.

For the single particle distribution we have ($\vec{B} = \vec{j}a$, $\vec{b} = \vec{\ell}a$)

$$\begin{aligned} G^{(1)}(\vec{B},Y;\ \vec{b},y) &= -\left(\bar{\phi}_0 P_j e^{-H(Y-y)} Z_\ell\, e^{-Hy} Q_0 \phi_0\right) \\ &= -\left(\phi\left[\{\sigma_{j-i}\}\right] e^{-H(Y-y)} Z_\ell\, e^{-Hy}\, \phi\left[\{\sigma_i\}\right]\right) \end{aligned} \tag{4.7}$$

with $\sigma_i = \delta_{i,0}$. Taking into account the equation of motion of the state $\phi[\sigma]$ we have

$$G^{(1)}(\vec{B},\ Y;\ \vec{b},\ y) = -\left(\phi\left[\{\sigma_{j-i}(Y-y)\}\right] Z_\ell\, \phi\left[\{\sigma_i(y)\}\right]\right) \tag{4.8}$$

and from 3.11 we obtain the final result

$$G^{(1)}(\vec{B},Y;\ \vec{b},y) = \sigma_{j-\ell}(Y-y)\sigma_\ell(y) \prod_{i \neq \ell} \left(1 - \sigma_{j-i}(y)\sigma_i(y)\right), \tag{4.9}$$

$\vec{B} = \vec{j}a$, $b = \vec{\ell}a$.

The behavior of this single particle amplitude can be obtained from the expression for $\sigma(b, y)$ in 4.5 and 4.6.

Let us consider first the case $x > 1$, where $\sigma(b, y)$ is a Regge pole with intercept smaller than one (see eq. 4.5). To the leading order we obtained from 4.9

$$G^{(1)}(\vec{B},Y;\ \vec{b},\ y) \approx \sigma(\vec{B} - \vec{b},\ Y - y)\sigma(\vec{b},\ y)$$

$$\simeq e^{2J(1-x)Y}\ \frac{e^{-(\vec{B} - \vec{b})^2/2Ja^2(Y-y)}}{(Ja^2(Y - y)^{D/2}}\ \frac{e^{-b^2/2Ja^2y}}{(Ja^2y)^{D/2}}\ , \qquad x < 1 \quad . \tag{4.10}$$

This amplitude corresponds to the production of the particle via the exchange of the Regge poles of this lattice theory as in Fig. 2. Nonleading contributions to 4.10, coming from the product in 4.9 and from corrections in 4.5, are given by Regge cuts.

Let us consider how the case $x < 1$, where $\sigma(\vec{b},\ y)$ is an expanding disc, eq. 4.6. In this case the expression in 4.9 is essentially different from zero in the configuration in which the two discs $\sigma(\vec{b},y)$ and $\sigma(\vec{B} - \vec{b},\ Y - y)$ do not overlap and are tangent, i.e., where (see Fig. 6)

$$b^2 \simeq v^2(x)y^2 \quad , \quad (\vec{B} - \vec{b})^2 \simeq v^2(x)(Y - y)^2$$

$$\vec{B} \cdot \vec{b} > 0 \quad . \tag{4.11}$$

In fact the product $\pi_{i \neq \ell}$ in 4.9 is different from zero if the two discs overlap only in a finite number of points, n, in the lattice

$$\pi_{i \neq \ell}\left(1 - \sigma_{j-i}(Y - y)\sigma_i(y)\right) = \left(1 - \sigma^2(x)\right)^{n-1} , \qquad (4.12)$$

i.e., in a region in the b space with zero measure in the continuum limit.

The spread around the points in 4.11 is given by the Gaussian tail of the disc in 4.6 and we have then

$$G^{(1)}(\vec{B},Y;\vec{b},y) \approx \sigma^2(x) \frac{e^{-\left(|b| - v(x)y\right)^2/2Ja^2y}}{(Ja^2y)^{D/2}} \frac{e^{-\left(\left|\vec{B}-\vec{b}\right| - v(x)(Y-y)\right)^2/2Ja^2(Y-y)}}{\left(Ja^2(Y-y)\right)^{D/2}} \qquad (4.12)$$

$$\theta\left(\vec{B}\cdot\vec{b}\right) .$$

For D = 1 and x = 0 this semiclassical approximation coincides with the exact result in 3.14. This gives further support for role of the semiclassica approximation as a reliable probe of the theory for different x and D.

Integrating 4.12 to have the differential cross section, we obtain

$$\frac{d\sigma}{dy} \approx \sigma^4(x) \frac{1}{\left((Y-y)y\right)^{D/2}} \qquad (4.13)$$

which generalizes to $x < 1$ and any D the result of the previous section. The physics of the process is then equivalent to the ones we discuss in the $x = 0$ $D = 1$ case.

The generalization to the n particle diffractive amplitudes is straightforwar in the case $x > 1$. In fact in this case the time evolution of the $\phi[\sigma]$ state is essentially given by the Regge pole propagator of eq. 4.5. It is easy to see, using the property

$$Z_j x^j_{\sigma_j} = \sigma_j \frac{d}{d\sigma_j} x^j_{\sigma_j} \tag{4.14}$$

and that $\sigma(by)$ is a Regge pole, that the leading contribution to $G^{(n)}$ is given by the perturbative form in Fig. 2 in which particles are emitted via the exchange of a simple Regge pole.

The calculation of $G^{(n)}$ for $x < 1$ is more complicated, and for $n > 1$ the case of $D > 1$ has some essentially different features than the case $D = 1$. The operator Z on the state $\phi[\sigma]$ gives

$$Z_{\ell_1} \phi[\sigma] = \phi[\sigma] - \phi_{\ell_1}[\sigma] \tag{4.15}$$

where the state ϕ_{ℓ_1} is obtained from ϕ by setting the field $\sigma_i = 0$ at $i = \ell_1$. As in the previous section we have a vanishing contribution to $G^{(n)}$ when the point ℓ_1 is well inside the disc of σ_i, due to the fact that the hole gets gradually washed away, while its position is unchanged (see Eq. 4.4). This feature presumably holds also if the hole is inside but close to the boarder, as long as the boundary condition, i.e., the shape of the holed disc, is smooth enough. The relevant contribution comes then again only when ℓ_1 is at the border of the disc, i.e.

$$|\vec{b}_1| = |\vec{\ell}_1 a| \simeq v(x) y_1 \tag{4.16}$$

and the state ϕ_{ℓ_1} can be represented as in Fig. 7. The difference between the D = 1 and D > 1 cases becomes clear from this figure. In fact for D = 1 the state ϕ is a box state and ϕ_{ℓ_1} is <u>also</u> a box state with a smaller length. The two states in 4.15 then evolve in the same way giving the same result for $G^{(n)}$ of the previous section, with a velocity given by $v(x) = Ja(1-x)^{\frac{1}{2}}$.

In the case D > 1 instead the state ϕ_{ℓ_1} is a disc with a hole at the border, which tends to move out in the process of evolution (see Fig. 7). This implies that the state 4.15, evolved in time

$$e^{-H(y_2 - y_1)} Z_{\ell_1} \phi[\sigma] = e^{-H(y_2 - y_1)} \left(\phi[\sigma] - \phi_{\ell_1}[\sigma]\right), \tag{4.17}$$

is for D > 1 exponentially dumped in $y_2 - y_1$. On the other hand the properties of alignment of the various $\vec{b}_j = \vec{\ell}_j a$ with $\vec{B} = \vec{i}\, a$ and the fact that a rapidity ordering implies an impact parameter ordering

$$|\vec{b}_j| \simeq v(x) y_j; \quad |\vec{B}| \simeq v(x) Y \tag{4.18}$$

remain even for D > 1. In fact in order not to have a zero matrix element of $G^{(n)}$, Z_{ℓ_1} has to act at the position where the hole, created by the previous Z_{ℓ_1}, is propagated; and so on.

The features of the diffractive inelastic amplitudes for $x < x_c$ can be then obtained with the following pictorial time evolution in the <u>b</u> space. The

initial particle at time $y = 0$ and $\underline{b} = 0$ create a pomeron which makes a disturbance on the vacuum state ϕ_0 at $\underline{b} = 0$ which propagates in time as a disc of radius $v(x)y$. This disc leads to the hadronic disc in the elastic process. However if a particle is diffractively emitted at time y_1 and $\underline{b}_1$, the corresponding mass operator can act only at the border of the disc expanded for y_1 time so that $b_1 \approx v(x)y_1$. As a result of this operation, we obtain a state corresponding to the original disc minus a state corresponding to the disc deformed by a hole at b_1 (Eq. 4.15). This hole remains at the border during the propagation. If another particle is diffractively emitted at y_2, $\vec{b}_2$ the mass operator must act again at the border of the expanded disc, i.e., $b_2 \simeq v(x)y_2$ and at the position of the propagated hole produced by the first particle so that $\vec{b}_1\vec{b}_2$ should be allowed. After this operation we remain with the difference of two states which again corresponds to the disc and the disc with a hole at b_2 so that the same mechanism works for all the other emitted particles. Finally we have that a pomeron has to be annihilated by the other interacting particles at Y and $\underline{B}$ and this can be done again only at the border of the disc $B = v(x)Y$ and at the position of the last propagated hole. As a result the rapidity differential cross sections are given by

$$\frac{d\sigma}{dy_1 \ldots dy_n} = \sigma^4(x) \frac{1}{(Y - y_n)^{D/2}} \prod_{i=2}^{n} g(y_i - y_{i-1}) \frac{1}{y_1^{D/2}}, \quad x < 1, \qquad (4.19)$$

where for D = 1, g(y) is decreasing as a power $y^{-3/2}$ while for D > 1 it is decreasing exponentially.

V. SUMMARY OF RESULTS AND PHYSICAL PICTURE

In the simple pole model the only diagrams contributing to inelastic fully diffractive production are the ladder-like diagrams appearing in Fig. 2. In that case the cross-section is given by

$$\frac{d\sigma}{dy_1 \ldots dy_n} = s^{\alpha_0 - 1} \prod_{i=1}^{n} \frac{1}{y_i} \tag{5.1}$$

where α_0 is greater or equal to one. Unitarity is clearly violated for any $\alpha_0 > 1$. However it was shown[6] that even for $\alpha_0 = 1$, s channel unitarity is violated. This happens because the Gaussian structure in impact parameter is reflected by a damping factor of only $1/y_i$ associated with each rapidity difference, y_i. Thus the resulting structure in rapidity will be that in which large gap configuration is favored. The introduction of absorptive effects in the form of the triple-pomeron interaction changed dramatically both the impact parameter and rapidity structure of these production processes, for the case $\alpha_0 \geq \alpha_c$.

For $\alpha_0 > \alpha_c$ (i.e., $x < x_c$) a peripheral picture emerges in impact parameter space. For a given set of rapidities y_i and total rapidity Y, a rigid positioning is imposed on the corresponding impact parameters. Each b_i is constrained to be at

$$b_i \approx v(x)y_i \; ; \qquad B \approx v(x)Y \quad . \tag{5.2}$$

Moreover all particles are alligned in the same direction. This is in sharp distinction both from the Gaussians of unabsorbed Regge poles and the disc structure of the fully absorbed elastic amplitude.

As a result of this depletion in impact-parameter phase space the differential cross-sections are damped in the rapidity gaps. We obtain

$$\frac{d\sigma}{dy_1 \ldots dy_n} \propto \sigma^4(x) \frac{1}{(Y - y_n)^{D/2}} \prod_{i=2}^{n} g(y_i - y_{i-1}) \frac{1}{(y_1)^{D/2}} \tag{5.3}$$

where for $D = 1$, $g(y)$ decreases like $1/y^{3/2}$, while for $D = 2$ the depletion is even stronger and $g(y)$ is exponentially decreasing. The rapidity structure of the absorbed cross-section (Eq. 5.3) is very different from the rapidity structure before absorption was taken into account (eq. 5.1). The damping in $g(y)$ is strong enough to cluster the produced particles. The leading configuration will eventually have as small as possible large gaps. The energy behavior of each σ_n is constant.

Turning to the contribution of these processes to the total cross-section, we find that it is constant in energy and its ratio to the total cross-section is vanishing, thus resolving the FK paradox. The absorptive effects turned out to be larger the larger the transverse dimension. It is interesting to note that in the extreme case $D = 0$, as long as α_0 (i.e. the gap Δ) is finite, the FK paradox will not occur due to the non-degeneracy of the ground state. In fact for very large α_0 the cross-section σ_n behaves as

$$\sigma_n = \frac{(\Delta Y)^n}{n!} e^{-2\Delta Y}. \qquad (5.4)$$

Thus only for n = 0 will the cross-sections be non-vanishing for $\Delta \to 0$. The FK paradox is avoided here without the help of b-space depletion.

For very large α_0 (i.e. x = 0) the model was exactly solvable, a semi-classical approximation enabled us to extend the results to $x \neq 0$ leading to Eq. (5.3). A signel for a change in character as x increases appears already in Eq. (5.3). In fact $\sigma(x)$, appearing in the equation, is the order parameter which vanishes as x tends to x_c.

We have not treated in the spin model the case $x = x_c$. This case, however, should smoothly join the distribution in (5.3) with the perturbative one (for $\alpha < 1$). This case was treated for the full RFT in ref. 7. The corresponding relation to eq. (5.3) is more complicated due to the fact that it does not simply factorize. Nevertheless it turns out the all rapidity intervals are damped, the leading configuration has only one large gap and the energy behavior of each σ_n is like that of σ_{el} which (in all approximations) decrease logarithmically by itself and constitutes a decreasing ratio of the total cross-section. It was also shown that the FK paradox does not arise even when summing over all multiplicities n. In this case increasing α_0 toward α_c one can trace the effects of the absorptive mechanism to the screening of the produced particle vertices. It would be interesting to understand exactly how this picture evolves when one decreases α_0 to α_c.

ACKNOWLEDGMENTS

We wish to thank W. Bardeen for very stimulating and critical discussions.

APPENDIX

In this Appendix we show for $D = 1$, $x = 0$, that in the evaluation of the $G^{(n)}$ amplitude, the mass operator Z_ℓ should act only at the border of the box states, thus leading to the y, b ordering and to the factorization of the cross sections.

Let us consider the contribution to $G^{(2)}$

$$G^{(2)} = \langle \bar{L}^j e^{-H(Y - y_2)} Z_{\ell_2} e^{-H(y_2 - y_1)} Z_{\ell_1} e^{-Hy_1} R^0 \rangle \tag{A.1}$$

$$= \sum_{n_1=0}^{\infty} \sum_{n_2=0}^{\infty} f_{\ell_1 + n_1}(y_1) f_{\ell_2 + n_2}(Y - y_2) \langle \bar{L}^{j - \ell_2 - n_2} Z_{\ell_2} e^{-H(y_2 - y_1)} Z_{\ell_1} R^{\ell_1 + n_1} \rangle .$$

The time evolution of the state $Z_{\ell_1} R^{\ell_1 + n_1}$ is different whether $n_1 = 0$ or $n_1 > 0$. In fact if $n_1 = 0$, the hole created by Z_{ℓ_1} is at the edge of the state R^{ℓ_1}

$$Z_{\ell_1} R^{\ell_1} = R^{\ell_1} - R^{\ell_1 - 1} , \tag{A.2}$$

thus the hole moves with the edge.

For $n_1 > 0$ the hole created by Z_{ℓ_1} inside the state $R^{\ell_1 + n_1}$ remains in the same position during the propagation. In fact the equation of motion is ($x = 0$)

$$HZ_\ell R^m = Z_\ell \left[J(R^m - R^{m+1}) + 2JR^m \right] \qquad m > \ell \tag{A.3}$$

which gives ($n_1 > 0$)

$$e^{-H(y_2 - y_1)} Z_{\ell_1} R^{\ell_1 + n_1} = e^{-2J(y_2 - y_1)} \sum_{m=0}^{\infty} f_m(y_2 - y_1) Z_{\ell_1} R^{\ell_1 + n_1 + m} . \tag{A.4}$$

This equation implies that the hole at ℓ_1 remains in the same position but it is exponentially filled up during the time evolution. Moreover it is easy to see that only the $m = 0$ term in A.4 is contributing to the matrix element $G^{(2)}$. Thus, the contribution in A.1 with $n_1 > 0$ is damped with respect to the contribution with $n_1 = 0$, we have kept in 3.24, by the factor

$$e^{-2J(y_2 - y_1)} f_0(y_2 - y_1) = e^{-3J(y_2 - y_1)} . \tag{A.5}$$

In fact, on the tail of the Poisson distribution we have $f_0(y) = e^{-Jy}$.

REFERENCES

[1] V. N. Gribov, Soviet Phys. JETP 26, 414 (1968); V. N. Gribov and A. A. Migdal, Soviet J. Nuclear Phys. 8, 583, 783 (1969).

[2] A. A. Migdal, A. M. Polyakov and K. A. Ter-Martirosian, Phys. Lett. 48B, 239 (1974); Soviet Phys. JETP 40, 420 (1974); H. D. I. Abarbanel and J. B. Bronzan, Phys. Lett. 48B, 345 (1974); Phys. Rev. D9, 2397 (1974).

[3] D. Amati, M. Ciafaloni, M. Le Bellac, and G. Marchesini, CERN preprint TH. 2152 (1976).

[4] D. Amati, M. Ciafaloni, G. Parisi, and G. Marchesini, CERN preprint TH. 2185 (1976).

[5] J. L. Cardy, SLAC preprint PUB-1784 (1976).

[6] I. A. Veriev, O. K. Kanchelli, S. G. Martirosyan, A. M. Popova, and K. A. Ter-Martirosian, Soviet Phys. JETP 19, 1146 (1964); J. Finkelstein and K. Kajantie, Nuovo Cimento 56A, 659 (1968); Phys. Lett. 26B, 305 (1968). Hereafter called FK.

[7] J. Bartels and E. Rabinovici, Phys. Rev. D12, 3938 (1975), J. Bartels and E. Rabinovici, Phys. Letters B58, 171 (1975).

[8] A. A. Migdal, A. M. Polyakov, and K. A. Ter-Martirosian, see Ref. 2. J. Bartels, Phys. Rev. D11, 2977 (1975).

[9] M. Ciafaloni, G. Marchesini and G. Veneziano, Nuclear Phys. B74, 493 (1975); P. Suranyi, Phys. Rev. D12, 2124 (1975); M. Ciafaloni and G. Marchesini, CERN preprint TH. 2146 (1976).

[10] V. Alessandrini, D. Amati and R. Jengo, CERN preprint TH. 2089 (1975).

[11] R. Jengo-Trieste preprint (1976); J. Bronzan, J. Shapiro and R. Sugar, Santa Barbara preprint (1976).

FIGURE CAPTIONS

Fig. 1: The state $\xi^{\ell,m}: \prod_{i<\ell} X_0^i \prod_{i=\ell}^{m} X_1^i \prod_{i>\ell} X_0^i$.

Fig 2: The ladder diagram representing $n+2$ particle production by multi-pomeron exchanges.

Fig. 3: a) - b) absorption corrections to simple multi-pomeron exchanges c) a new production process induced by the triple pomeron coupling.

Fig. 4: Contributions to the production process in which more than one pomeron is attached to the external particle.

Fig. 5: The states $\xi^{-n,n'}$ and $\bar{\xi}^{i'-m,i'+m'}$ between which the transition element of the mass insertion operator, Z_ℓ, is calculated in Eq. (3.4).

Fig. 6: In the case $\sigma_{2\to3}$, for $D=2$ a produced particle with rapidity y will have an impact parameter $b \approx Vy$. All particles are alligned in impact parameter.

Fig. 7: At $D=2$ a state with a curvature at the edge evolves into a complete disc, with the "dent" at the edge disappearing, this behaviour is different for $D=1$.

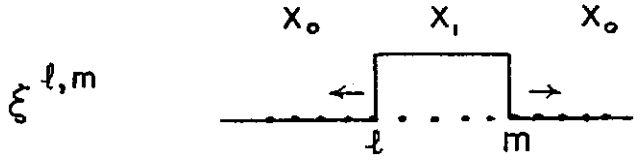

Fig. 1

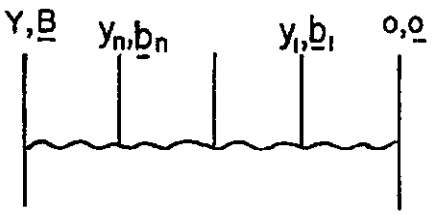

Fig. 2

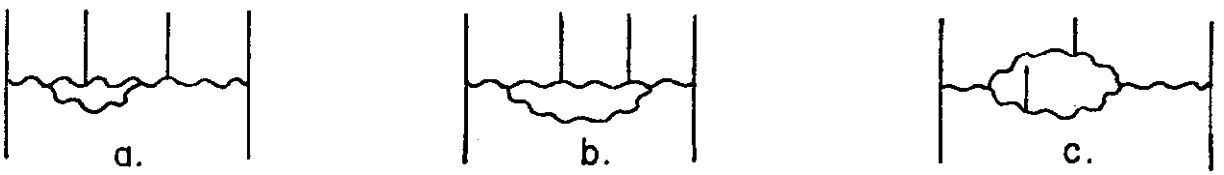

Fig. 3

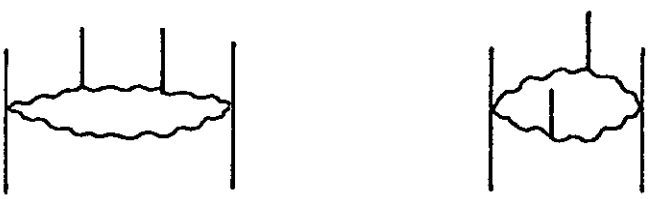

Fig. 4

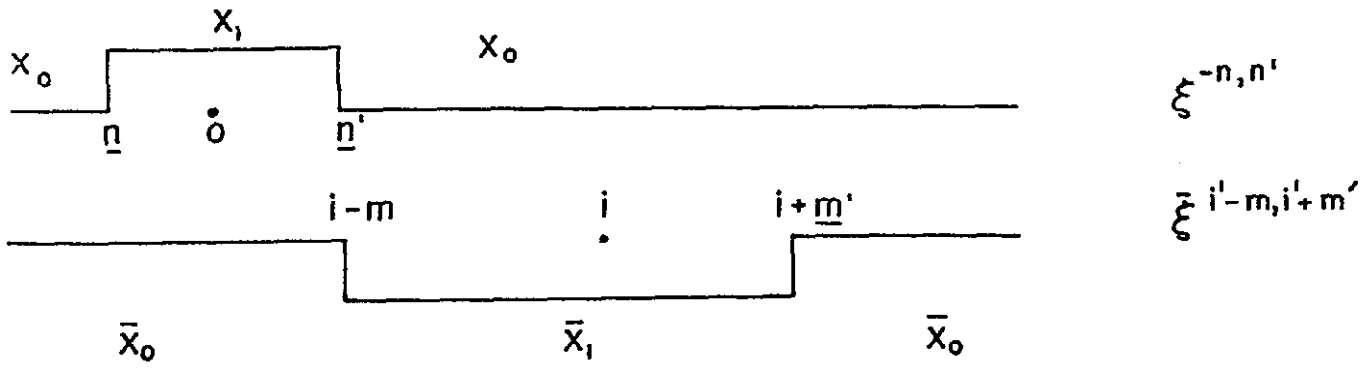

Fig. 5

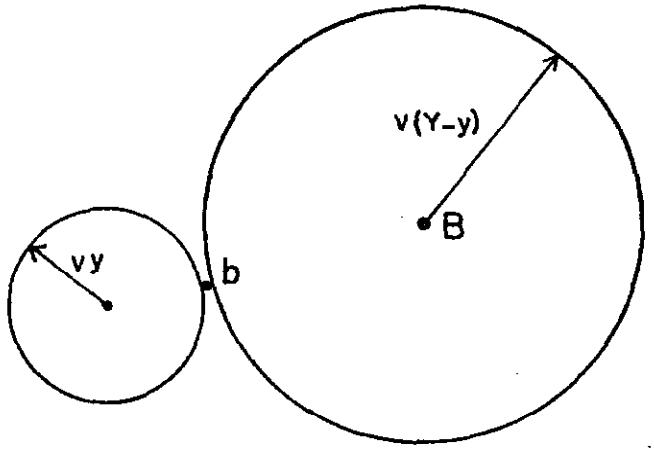

Fig. 6

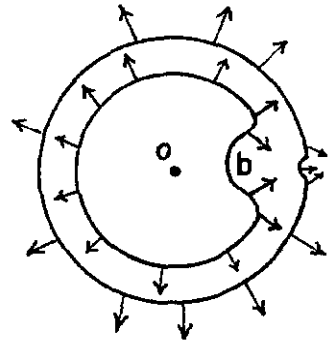

Fig. 7